A class of synaptic signaling molecules required for homeostatic potentiation also tunes homeostatic depression

Catherine J. Yeates[1,2,4], C. Andrew Frank[1,2,3]

[1] Department of Anatomy and Cell Biology, University of Iowa Carver College of Medicine, Iowa City, IA, USA

[2] Interdisciplinary Graduate Program in Neuroscience, University of Iowa, Iowa City, IA, USA

[3] Iowa Neuroscience Institute, University of Iowa Carver College of Medicine, Iowa City, IA, USA

[4] Present Address: Department of Biology, University of Dayton, Dayton, OH, USA

*** Correspondence:**
C. Andrew Frank
andy-frank@uiowa.edu

Keywords: synapse, homeostasis, depression, *Drosophila melanogaster*, NMJ, neurotransmission, plasticity

Abstract

Synapses and circuits rely on homeostatic forms of regulation in order to transmit meaningful information. The *Drosophila melanogaster* neuromuscular junction (NMJ) is a well-studied synapse that shows robust homeostatic control of function. Most prior studies of homeostatic plasticity at the NMJ have centered on presynaptic homeostatic potentiation (PHP). PHP happens when postsynaptic muscle neurotransmitter receptors are impaired, triggering retrograde signaling that causes an increase in presynaptic neurotransmitter release. As a result, normal levels of evoked excitation are maintained. The counterpart to PHP at the NMJ is presynaptic homeostatic depression (PHD). Overexpression of the Drosophila vesicular glutamate transporter (VGlut) causes an increase in the amplitude of spontaneous events. PHD happens when the synapse responds to the challenge by decreasing quantal content during evoked neurotransmission – again, resulting in normal levels of postsynaptic excitation.

We hypothesized that there may exist a class of molecules that affects both PHP and PHD. Impairment of any such molecule could hurt a synapse's ability to respond to any significant homeostatic challenge. We conducted an electrophysiology-based screen for blocks of PHD. While we did not observe a block of PHD in the genetic conditions screened, we instead found loss-of-function conditions that led to excess depression – i.e., a substantial deficit in evoked amplitude when combined with VGlut overexpression. The conditions causing this phenotype included a double heterozygous loss-of-function condition for genes encoding the inositol trisphosphate receptor (IP_3R – *itpr*) and ryanodine receptor (*RyR*). IP_3Rs and RyRs gate calcium release from intracellular stores. Pharmacological agents targeting IP_3R and RyR recapitulated the genetic losses of these factors, as did lowering calcium levels from other sources. Our data are consistent with the idea that some factors required for homeostatic potentiation are also required for the synapse to achieve appropriate levels of homeostatic depression. Loss of such factors may disorient compensatory plasticity signals.

1 Introduction

Animal nervous systems use forms homeostatic synaptic plasticity to maintain stable function. Over the last 20-25 years, studies from diverse systems have revealed a wealth of information about how forms of homeostatic synaptic plasticity are implemented (Davis, 2013; Davis and Müller, 2015; Delvendahl and Müller, 2019; Marder and Goaillard, 2006; Pozo and Goda, 2010; Turrigiano, 2008). In particular, the *Drosophila melanogaster* neuromuscular junction (NMJ) has uncovered many facets of homeostatic implementation on a molecular level (Frank, 2014a; Frank et al., 2020). Much of the NMJ homeostasis work in both Drosophila and vertebrates has focused on a form of homeostatic plasticity termed presynaptic homeostatic potentiation (PHP). With PHP, manipulations that impair postsynaptic muscle receptor function trigger an increase in presynaptic vesicle release (Cull-Candy et al., 1980; Davis et al., 1998; Frank et al., 2006; Petersen et al., 1997; Wang et al., 2016).

Homeostatic plasticity the NMJ is a bi-directional process. First, PHP is reversible – when manipulations that impair muscle receptor function are removed, the presynaptic potentiation ceases (Wang et al., 2016; Yeates et al., 2017). Second, the Drosophila NMJ can depress quantal content in a homeostatic manner functionally opposite to PHP: Presynaptic homeostatic depression (PHD) happens when there is a decrease in quantal content in response to a perturbation causing an increase in quantal size. Experimentally, one way to trigger PHD is to overexpress the *Drosophila* vesicular glutamate transporter gene, *VGlut,* in motor neurons. Overexpression of the glutamate transporter leads to an increase in the diameter of glutamatergic vesicles, an increase in quantal size across the entire distribution of spontaneous miniature events, and very large spontaneous quantal events (Daniels, 2004). To compensate for this, quantal content at the NMJ is lowered, resulting in normal evoked postsynaptic excitation (Daniels et al., 2004).

Many genes have been shown to be necessary for PHP at the NMJ. But much less is known about PHD. PHP and PHD result in opposite changes in quantal content, and studies suggest divergent and separable mechanisms governing these forms of homeostatic plasticity. Some genes required for homeostatic potentiation are dispensable for homeostatic depression (Gaviño et al., 2015; Li et al., 2018; Marie et al., 2010). Moreover, unlike homeostatic potentiation, homeostatic depression does not appear to involve a change in the size of the readily releasable pool of synaptic vesicles. Rather, homeostatic depression appears to involve a decrease in release probability (Gaviño et al., 2015). Finally, PHP at the NMJ appears to be a process that is dependent the input (i.e. the type of synapse formed at the NMJ) while PHD does not appear to be input specific (Li et al., 2018).

The degree of overlap between homeostatic depression and homeostatic potentiation is unknown. We designed a small-scale, directed screen to test for links between these two forms of homeostatic plasticity. For the screen, we targeted genes based on prior evidence that their impairment in the neuron caused a failure of the long-term maintenance of PHP. We examined loss-of-function conditions for these genes in a VGlut overexpression background for PHD. We did not find any cases of failed homeostatic depression – the conditions we examined showed decreases in quantal content in response to increased quantal size. However, we did find an interesting and unexpected evoked neurotransmission phenotype: a robust decrease in excitatory postsynaptic potential (EPSP) amplitude in a VGlut overexpression background because of a profound decrease in quantal content (QC). We observed this phenotype for a double heterozygous loss-of-function condition for the Ryanodine and IP_3 receptors. In our follow-up work, pharmacology phenocopied this genetic result, and our overall findings are consistent with the idea that the PHD system may show a heightened sensitivity to low calcium.

Prior characterizations of homeostatic depression did not report decreases in EPSP amplitude in VGlut overexpression relative to controls. Studies at the NMJ generally suggest models in which homeostatic compensation generally maintains evoked neurotransmission at the synapse approximately at control levels (Davis, 2013). Our results suggest that perturbation of calcium regulation may result in a defect in tuning homeostatic responses to maintain EPSPs at control levels.

2 Materials and Methods

Drosophila stocks and husbandry

Fruit fly stocks were obtained from the Bloomington Drosophila Stock Center (BDSC, Bloomington, Indiana), Kyoto Stock Center (DGRC, Kyoto, Japan), Japan National Institute of Genetics (Mishima, Shizuoka, Japan), Vienna Drosophila Research Center (VDRC, Vienna, Austria), or from the labs that generated them. w^{1118} was used as a wild-type (WT) control (Hazelrigg et al., 1984). RNAi lines and mutants used in the screen are reported in Supplemental Table S1.

Fruit flies were raised on cornmeal, molasses, and yeast medium (see BDSC website for standard recipe) in temperature-controlled conditions. Animals were reared at 25°C until they reached the wandering third instar larval stage, at which point they were selected for electrophysiological recording. *UAS-VGlut* (Daniels et al., 2004) was recombined with *OK371-GAL4* (Mahr and Aberle, 2006; Meyer and Aberle, 2006) to drive constitutive overexpression of VGlut. The full genotype of these animals is: *w; VGlut, OK371-Gal4/CyO-GFP*. Virgins of these flies were crossed to RNAi lines or mutants to test for changes to homeostatic depression. *w; OK371-Gal4/+* was used as a genetic control for baseline electrophysiology.

Electrophysiology and analysis

Larvae were dissected in a modified HL3 saline comprised of: NaCl (70 mM), KCl (5 mM), $MgCl_2$ (10 mM), $NaHCO_3$ (10 mM), sucrose (115 mM = 3.9%), trehalose (4.2 mM = 0.16%), HEPES (5.0 mM = 0.12%), and $CaCl_2$ (0.5 mM, except as noted).

For pharmacology, Dantrolene (R&D Systems) and Xestospongin C (Abcam) were used. Dantrolene was mixed into saline to a final concentration of 25 µM. Larvae were cut open on the dorsal side and allowed to incubate in the Dantrolene saline for 5 minutes. The rest of the dissection and recording was completed in Dantrolene saline. Xestospongin C was applied in a similar manner, with the animals allowed to incubate in 20 µM Xestospongin C saline for 5 minutes before they were recorded, also in saline containing Xestospongin C.

Electrophysiological data were collected using an Axopatch 200B amplifier (Molecular Devices, Sunnyvale, CA) in bridge mode, digitized using a Digidata 1440A data acquisition system (Molecular Devices), and recorded with pCLAMP 10 acquisition software (Molecular Devices). A Master-8 pulse stimulator (A.M.P. Instruments, Jerusalem, Israel) and an ISO-Flex isolation unit (A.M.P. Instruments) were utilized to deliver 1 ms suprathreshold stimuli to the appropriate segmental nerve. The average spontaneous miniature excitatory postsynaptic potential (mEPSP) amplitude per NMJ was quantified by hand, approximately 100 individual spontaneous release events per NMJ (MiniAnalysis, Synaptosoft, Fort Lee, NJ). Measurements from all NMJs of a given condition were then averaged. For evoked neurotransmission, 30 excitatory postsynaptic potentials (EPSPs) were averaged to find a value for each NMJ. These were then averaged to calculate a value for each condition. Quantal content (QC) was calculated by the ratio of average EPSP and average mEPSP amplitudes for each individual NMJ. An average quantal content was then calculated for each condition. EPSP variability was assessed by measuring each of the 30 traces individually and calculating a standard deviation and range for that NMJ. Range was defined as the maximum EPSP value minus the minimum EPSP value.

Statistical Analyses

Statistical analyses were conducted using GraphPad Prism Software. Statistical significance was assessed either by Student's T-Test when one experimental data set was being directly compared to a control data set, or one-way ANOVA with Tukey's post-hoc test when multiple data sets were being compared. Specific p value ranges are noted in the Figure legends and shown in graphs as follows: * $p < 0.05$, ** $p < 0.01$, and *** $p < 0.001$ (* and # are used in Figures if there are additional comparisons highlighted). For some comparisons that are close to $p < 0.05$ statistical significance but do not achieve it ($0.05 < p < 0.1$), specific values are reported on the graph itself. Calcium cooperativity data were analyzed using a non-linear fit regression analysis on GraphPad Prism.

3 Results

A recombinant line to analyze presynaptic homeostatic depression (PHD)

Using previously published reagents, we generated a fly stock with constitutive *VGlut* transgene overexpression. Such a stock could be used as a tool for a single-cross genetic screen. To generate the stock, we recombined the *OK371-Gal4* motor neuron driver (Mahr and Aberle, 2006; Meyer and Aberle, 2006) with a *UAS-VGlut* transgene (Daniels et al., 2004). We placed these two genetic elements in *cis* on *Drosophila melanogaster* Chromosome II. *OK371-Gal4* is an enhancer trap line for the *VGlut* promoter itself. This ensured that GAL4-driven *UAS-VGlut* overexpression would happen in desired tissues, *Drosophila* motor neurons.

We tested if the recombinant line constitutively overexpressing *UAS-VGlut* could express PHD at the NMJ. We crossed the recombinant stock to our wild-type stock (w^{1118}, herein: WT) (Cross result,

herein: "*VGlut, OK371/+*"). By NMJ electrophysiology, we recorded from WT control, *OK371/+* control, and *w; VGlut, OK371/+*. As expected, *VGlut, OK371/+* NMJs showed an increase in spontaneous miniature excitatory postsynaptic potential (mEPSP) amplitude compared to controls (Fig. 1A-C). Compared to WT control NMJs, there was no significant difference in evoked postsynaptic amplitudes for *VGlut, OK371/+* NMJs (Fig. 1D). This was because of an accurate homeostatic decrease in quantal content (QC) (Fig 1E) – hence, successful PHD. This result matched prior studies that had used WT as a control and a *trans OK371/UAS-VGlut* combination to induce PHD (Daniels et al., 2004; Gaviño et al., 2015; Li et al., 2018).

Even though PHD was successful relative to WT for our test cross, we noted a small, but statistically significant, baseline increase in the EPSP amplitude of *OK371/+* NMJs. This increase in *OK371/+* EPSP level was present compared either to WT control or to *VGlut, OK371/+* (Fig. 1D). One possibility is that the *OK371/+* genetic background has slightly elevated release, and the combined addition of *UAS-VGlut* reveals a slight depression in evoked amplitude. Noting this potentially important difference in our driver control, we continued using the *OK371/+* heterozygous condition as a genetic background control. *OK371/+* is a closer genetic control for PHD analysis than WT.

A genetic screen suggests a role for calcium stores in homeostatic depression

We used our recombinant line to conduct a genetic screen for conditions that affect presynaptic homeostatic depression (PHD). We crossed the recombinant stock to *UAS-RNAi* stocks and we selected larvae for recording (Materials and Methods, Fig. 2A). For the screen, we targeted a subset of genes previously identified as in the neuron for homeostatic potentiation, or closely related genes. We tested 43 genotypes (sometimes multiple conditions for a single gene), including our homeostatic depression condition, *VGlut, OK371/+* (Fig. 2B, C).

The aggregate results of the screen are reported here (Fig. 2B, C; raw data in Supplementary Table S1). We recorded from 42 experimental heterozygous *mutant/+* or > *UAS-RNAi/+* conditions, in the *VGlut, OK371/+* genetic background. Of those 42, 12 achieved EPSPs that were numerically larger than *VGlut, OK371/+*, and 22 achieved QCs that were numerically larger than *VGlut, OK371/+* (Fig. 2B, C). Increased evoked potentials could signify failed PHP – however, none of these cases represented statistically significant increases compared to *VGlut, OK371/+*. None were so much bigger than they were good candidates for "failed PHD." Indeed, all of the candidates had average EPSP and QC levels below *OK371/+* NMJ baseline recordings (Compare Figs 1D, E and Fig. 2B, C).

We noted a phenotype distinct from what we were initially seeking: two crosses yielded larvae with striking decreases in NMJ EPSP amplitudes, more than two standard deviations below the average EPSPs from the baseline *VGlut, OK371/+* data set (Fig. 2B). One case was knockdown of the *Survival motor neuron* (*Smn*) gene with the *UAS-Smn[RNAi]*^{JF02057} line in the *VGlut, OK371/+* background. This was intriguing because Drosophila *Smn* is homologous to human *SMN*. Defects in *SMN* cause Spinal Muscular Atrophy (Lefebvre et al., 1995). Drosophila Smn has been characterized as a potential model for Spinal Muscular Atrophy (Raimer et al., 2020; Sen et al., 2011; Spring et al., 2019). Smn has also previously been implicated in PHP (Sen et al., 2011). However, the result for *UAS-Smn[RNAi]*^{JF02057} was not replicated by other *Smn* knockdown or loss-of-function mutant test crosses (Fig. 2B, C). We did not follow up on *Smn* for this study.

A second case with a striking decrease in EPSP amplitude in the screen was a double heterozygous genetic condition in genes encoding the Drosophila Ryanodine receptor (*RyR*) and inositol 1,4,5-trisphosphate (IP_3) receptor (*itpr*): *VGlut, OK371/RyR*^{E4340K}*; itpr*^{90B}*/+* (Fig. 2B, C). Ryanodine receptors (RyRs) and IP_3 receptors (IP_3Rs) are localized to the endoplasmic reticulum. They mediate release of calcium from intracellular stores (Berridge, 1984, 1987, 1998; Simkus and Stricker, 2002). The

188 *RyR^{E4340K}* mutation is a single amino acid substitution (glutamic acid to lysine) (Dockendorff et al.,
189 2000), and the *itpr^{90B}* mutation is null mutant generated by imprecise excision of a transposon
190 (Venkatesh and Hasan, 1997). We previously defined a roles for RyR, IP_3R, IP_3 signaling and upstream
191 components in maintaining presynaptic homeostatic potentiation (PHP) (Brusich et al., 2015; James et
192 al., 2019).

193 In parallel, we screened single mutant manipulations for both genes. Neither the *RyR^{E4340K}/+* heterozy-
194 gous condition, nor the *itpr^{90B}/+* heterozygous condition – nor had any other single heterozygous or
195 RNAi knockdown conditions in either gene – yielded as significantly depressed EPSPs in response to
196 PHD challenge (Fig. 2B, C). Therefore, the screen result with the double heterozygote could be due to
197 a genetic interaction, or it could be due to other factors in the genetic background. This preliminary
198 finding required further characterization.

199 We tested if the electrophysiological phenotype could be due to a baseline neurotransmission defect
200 when both genes are heterozygous. By electrophysiology, we compared NMJs from *OK371/RyR^{E4340K};*
201 *itpr^{90B}/+* larvae as a baseline double heterozygous condition vs. NMJs from *VGlut, OK371/RyR^{E4340K};*
202 *itpr^{90B}/+* larvae (Fig. 3A-D). Just like WT, the baseline double heterozygous condition did have a slight
203 decrease in EPSP amplitude compared to *OK371/+* driver control (Fig. 3A). This indicated a small,
204 but discernible defect in neurotransmission in animals where the IP_3Rs and RyRs are both impaired.
205 Yet the double heterozygous condition with concurrent *VGlut* gene overexpression showed a lot of
206 depression compared to its own genetic control – increased quantal size (Fig. 3B), but markedly de-
207 creased evoked amplitude (Fig. 3C) because of a large decrease in quantal content (Fig. 3D), hence
208 "excess" PHD.

209 We noted that the EPSP amplitude in individual *VGlut, OK371/RyR^{E4340K}; itpr^{90B}/+* NMJ recordings
210 appeared to vary markedly from stimulus to stimulus. High variability could indicate unstable neuronal
211 excitability or release. To check if evoked release events were indeed more variable, we completed two
212 additional analyses. First, we extracted the amplitude of each individual EPSP event at every NMJ
213 recorded. From this information, we calculated the EPSP standard deviation (S.D.) per individual NMJ.
214 We also calculated a range for each NMJ by subtracting the maximum EPSP of the thirty from the
215 minimum. We averaged these S.D. and range measures for each genotype, considering all of the indi-
216 vidual EPSP recordings.

217 For both of these EPSP variability parameters, *w; VGlut, OK371/RyR^{E4340}; itpr^{90B}/+* animals showed
218 statistically significant higher standard deviations and ranges compared to controls (Fig. 3E). By con-
219 trast, double heterozygous baseline *OK371/RyR^{E4340K}; itpr^{90B}/+* NMJs did not differ significantly from
220 *w; OK371/+* driver control NMJs, suggesting that the variability stems from *VGlut* overexpression in
221 the mutant background (Fig. 3E). *w; VGlut, OK371/+* NMJs showed numerically higher variability
222 than *w; OK371/+*, but this was not statistically significant (Fig. 3E).

223

224 ***Pharmacology targeting Ryanodine and IP_3 receptors recapitulates loss-of-function genetics***

225 We tested if the electrophysiological phenotypes we observed genetically could be recapitulated by
226 combining genetics and pharmacology. We started with the drug Dantrolene. Dantrolene is a RyR an-
227 tagonist (Vazquez-Martinez et al., 2003; Zhao et al., 2001). In prior work at the *Drosophila* NMJ, we
228 found that application of Dantrolene can abrogate the long-term maintenance of PHP (James et al.,
229 2019).

230 For our first test with Dantrolene, we used a sensitized *OK371/+; itpr^{90B}/+* genetic background. With
231 this background, we could pharmacologically impair RyRs while genetically impairing IP_3Rs. We ap-
232 plied 25μM of Dantrolene to: 1) *OK371/+* NMJs; 2) *VGlut, OK371/+* NMJs; 3) *OK371/+; itpr^{90B}/+*

233 NMJs; and 4) *VGlut, OK371/+; itpr^{90B}/+* NMJs. The mEPSP amplitudes in both *VGlut*-overexpressing
234 lines were elevated compared to their respective controls (Fig. 4A). This indicated that in the presence
235 of Dantrolene, there was still homeostatic pressure that could induce PHD. EPSP amplitudes in both
236 *VGlut*-overexpressing lines were significantly decreased compared to their respective genetic controls
237 (Fig. 4B). This was because of a marked decrease in QC (Fig. 4A). Moreover, the *VGlut, OK371/+;*
238 *itpr^{90B}/+* condition with Dantrolene had significantly decreased evoked transmission compared to
239 *VGlut, OK371/+* with Dantrolene (Fig. 4A, B). This indicated a cumulative effect of impairing both
240 the IP_3Rs and RyRs in a PHD-challenged background.

241 It is possible that strong impairment of RyRs was sufficient to disorient the PHD regulation system.
242 We ran additional pharmaco-genetic tests with Dantrolene, this time using a second sensitized genetic
243 background, *OK371/RyR^{E4340K}* – with and without a *UAS-VGlut* overexpression. Again, mEPSPs were
244 evoked potentials became significantly larger when *VGlut* was overexpressed (Fig. 5A, left), but EPSPs
245 were significantly down (Fig. 5A, middle) because of a marked decrease in quantal content (Fig. 5A,
246 right).

247 Finally, we attempted the inverse pharmaco-genetic experiment from that in Figure 4. This time we
248 used the IP_3R inhibitor, Xestospongin C (Gafni et al., 1997; Wilcox et al., 1998) and the sensitized
249 *OK371/RyR^{E4340K}* genetic background. We applied 20 µM Xestospongin C, both to *OK371/RyR^{E4340K}*
250 NMJs and to *VGlut, OK371/RyR^{E4340K}* NMJs. The mEPSPs were numerically larger when *VGlut* was
251 overexpressed (Fig. 5B, left) – though this time, for the Xestospongin C dataset, the data did not achieve
252 statistical significance for mEPSP size ($p = 0.10$). This could indicate weak homeostatic pressure in the
253 presence of Xestospongin C. Nevertheless, EPSPs were significantly down (Fig. 5B, middle) because
254 of a marked decrease in quantal content (Fig. 5B, right).

255 Taking our data together, for each case where we examined a dual impairment of RyR and IP_3R the
256 EPSP amplitudes and QC were all quite low with concomitant VGlut overexpression (Figs. 3-5). These
257 results are consistent with excess depression.

258

259 ***Excess PHD in very low extracellular calcium***

260 We wondered how impairment of channels that mediate release of calcium from intracellular stores
261 might cause the electrophysiological phenotypes that we observed. Our prior work suggested that these
262 ER calcium store channels and the signaling systems that control them are required to maintain home-
263 ostatic potentiation throughout life (Brusich et al., 2015; James et al., 2019). We also found a related
264 result: impairing Ca^{2+} store release mollified hyperexcitability phenotypes caused by gain-of-function
265 Ca_V2 amino-acid substitutions in the alpha1 subunit Cacophony. Ca_V2 channels mediate synaptic cal-
266 cium influx at the NMJ (Brusich et al., 2018). In light of these prior data, we considered two possibil-
267 ities for PHD. One model is that the IP_3R and RyR channels play a role in orienting PHD and ensuring
268 a proper level of depression. A different model is that calcium itself plays the important role. If this
269 latter idea were true, it might be the case that lowering calcium influx into the synaptic cleft would also
270 be sufficient to disorient the PHD system, resulting in excess depression.

271 As a test, we measured release over a range of low extracellular calcium concentrations (0.2-0.5 mM).
272 We examined six genotypes: 1) WT; 2) *w; OK371/+* ; 3) *w; VGlut, OK371/+*; 4) *w; RyR^{E4340K}/+;*
273 *itpr^{90B}/+*; 5) *w; OK371/RyR^{E4340K} ; itpr^{90B}/+*; and 6) *w; VGlut, OK371/RyR^{E4340K} ; itpr^{90B}/+*. To organ-
274 ize data and to calculate calcium cooperativity, we plotted quantal content as a function of calcium
275 concentration, with the x-y axes on a log-log scale (Fig. 6A, B). To account for different Ca^{2+} driving

forces in the different concentrations, we corrected QC for nonlinear summation in our plots and in our subsequent analyses (NLS Corrected QC) (Martin, 1955).

Non-linear regression analyses revealed that there was not a significant difference in calcium cooperativity between any of these genotypes over the range of extracellular [Ca^{2+}] we tested (Fig. 6A, B). The calculated log-log slope values of the control PHD genotypes were: WT (log-log slope = 1.810), *w; OK371/+* (log-log slope = 1.884), and *w; VGlut, OK371/+* (log-log slope = 2.117). Comparing those three slopes with one another by nonlinear regression yielded no significant difference in slope (p = 0.91). The log-log slope values of the double heterozygous conditions were: *w;* RyR^{E4340K}*/+ ;* $itpr^{90B}$*/+* (log-log slope = 1.737), *w;* $OK371/RyR^{E4340K}$*;* $itpr^{90B}$*/+* (log-log slope = 2.102), and *w; VGlut,* $OK371/RyR^{E4340K}$ *;* $itpr^{90B}$*/+* (log-log slope = 1.601). Comparing those slopes with one another also yielded no significant difference (p = 0.77).

Even though there was no significant difference in calcium cooperativity of release over the range of low [Ca^{2+}] conditions examined, our data did show a very large drop in release between 0.3 and 0.2 mM [Ca^{2+}] – specifically for the genotypes where PHD was induced by *UAS-VGlut* overexpression, or for the genotypes with a double heterozygous impairment of *RyR* and *itpr*. Examining the raw data at 0.2 mM [Ca^{2+}], we observed that there was significant homeostatic pressure for PHD signified by mEPSP amplitude increases in the VGlut-overexpression background (Fig. 6C, left). Yet except for the control NMJs, EPSP amplitudes were very much diminished (Fig. 6C, middle) because of stark drops in QC (Fig. 6C, right).

Together, the data point to two conclusions. First, low extracellular calcium on its own appears to be a case where the synapse experiences "excess" PHD (Fig. 6C, *VGlut, OK371/+* data). Second, double heterozygous impairment of *RyR* and *itpr* appears to cause very low levels of baseline release in low calcium, irrespective of PHD challenge (Fig. 6C, middle; compare with Fig. 3C). Taken together, these data suggest that lowering presynaptic calcium by any means (impairing store release and/or impairing influx) is sufficient to disorient the homeostatic set point for release.

Excess PHD with impaired Ca_V2 ***function***

As a final test of the idea depressed presynaptic calcium causes excess PHD, we turned to genetics. Drosophila Ca_V2 channels mediate synaptic calcium influx at the NMJ. We used a hypomorphic mutant in the Ca_V2 alpha1 subunit-encoding *cacophony* gene, cac^S, to limit calcium influx. Ca_V2 is essential for viability, but cac^S hypomorphs are viable and fertile (Kawasaki et al., 2000; Smith et al., 1998). Prior work showed that the cac^S homozygous condition dampens NMJ EPSP amplitude by about 70-80% (Frank et al., 2006); calcium imaging data suggest this is due to a ~50% decrease in Ca^{2+} influx during evoked stimulation (Müller and Davis, 2012). Beyond this phenotype in baseline neurotransmission, cac^S hypomorphs also block PHP expression and PHP-associated increases in presynaptic calcium influx (Frank et al., 2006; Müller and Davis, 2012).

With a single cross, we generated hemizygous cac^S*/Y; VGlut, OK371/+* male larvae (Fig. 7A). Compared to cac^S*/Y* as a baseline mutant control, cac^S*/Y; VGlut, OK371/+* NMJs have a marked increase in mEPSP size (Fig. 7B), indicating homeostatic pressure to induce PHD (Fig. 7B). However, comparing evoked potentials of those two conditions shows that cac^S*/Y; VGlut, OK371/+* NMJs have much smaller EPSPs (Fig. 7C). This was because of an extreme decrease in QC (Fig. 7D) – or "excess" PHD.

4 Discussion

We began this study in search of genetic conditions that affect PHD (Fig. 2). While we did not find any conditions that result in a block of PHD, we did find conditions that disrupt the tuning of PHD and

provide insight into the role calcium regulation plays in this form of homeostatic plasticity. When IP_3R and RyR functions are partially impaired – either by genetics or by pharmacology – the NMJ still executes a PHD-like process. But that process goes beyond what is appropriate for the homeostatic pressure that is applied to the system. As a result, evoked potentials at the NMJ are much smaller than baseline (Figs. 3-5). A similar "excess depression" phenotype is observed when extracellular [Ca^{2+}] is lowered to 0.2 mM (Fig. 6) and when the Ca_V2 alpha1 subunit gene *cacophony* harbors a hypomorphic mutation, cac^S (Fig. 7).

This phenotype has important implications for proper homeostatic control of synapse function. Taking our data together, we propose that presynaptic calcium plays an important role in tuning PHD to the appropriate level. Perturbations that dampen calcium efflux from stores or perturbations that dampen calcium influx from the extracellular environment can both disrupt PHD tuning (Fig. 8).

Known roles for calcium in tuning homeostatic plasticity

The notion that calcium plays a role in homeostatic signaling is not new. Many roles for voltage-gated calcium channels in synaptic homeostasis are well-documented (Frank, 2014a, b). Prior to our study, there was evidence for voltage-gated calcium channel regulation for both NMJ PHP and PHD. For PHP, loss-of-function conditions in Ca_V2/*cacophony* can impair or block this form of homeostatic regulation (Frank et al., 2006; Frank et al., 2009; Müller and Davis, 2012; Spring et al., 2016). Calcium imaging experiments suggest that the reason is because an increase in calcium influx through Ca_V2 is required for the upregulation of quantal content during PHP, and mutant conditions like cac^S block this increase (Müller and Davis, 2012). Recent studies report that Cacophony and other active zone protein levels increase at the NMJ active zone in response to PHP homeostatic challenges (Böhme et al., 2019; Goel et al., 2019; Gratz et al., 2019). And work from mammalian systems mirrors these findings. For example, with mouse hippocampal cultures, TTX exposure induces a homeostatic decrease in presynaptic calcium influx (Zhao et al., 2011).

The converse appears true for PHD. Calcium imaging data from two different studies has shown a decrease in the size of calcium transients at the NMJ in response to presynaptic nerve firing in VGlut-overexpressing animals (Gaviño et al., 2015; Li et al., 2018). The data are mixed on how these decreased transients might come about during PHD. Using a tagged *UAS-cacophony* cDNA transgene, two studies verified there was a reduction in the amount GFP-tagged Cacophony alpha1 subunits in Ca_V2 in a VGlut-overexpressing background (Gaviño et al., 2015; Gratz et al., 2019) However, one of these same studies demonstrated that if a tagged genomic construct is used instead, that same Ca_V2 reduction is not observed (Gratz et al., 2019). Since the transgenic tagged Cacophony-GFP is the product of a single *cac* splice isoform (Kawasaki et al., 2002; Kawasaki et al., 2004), it could be the case that some isoforms are more dynamically trafficked at the synapse. Another possibility is that existing active zone components are somehow modulated during PHD. Regardless of the actual mechanism, the phenomenon appears conserved: again, with rodent hippocampal preparations, increased neuronal activity through gabazine exposure induces a PHD-like phenomenon ultimately resulting in decreases in calcium influx and release (Jeans et al., 2017; Zhao et al., 2011).

Similarities and differences with prior PHD studies at the NMJ

We were able to conduct a PHD screen using our recombinant stock with the *UAS-VGlut* and *OK371-Gal4* elements on the same chromosome. We acknowledge that this type of *cis* strain construction is an unorthodox choice for Drosophila genetics. This is because *UAS-VGlut* is continually overexpressed

every generation. In principle, such a stock can pick up modifier mutations. The trade-off for our work was a simplified, single-generation crossing scheme for genetic screens. As it turns out, our recombinant stock with the driver and *UAS* elements in *cis* maintains consistent PHD challenge from generation to generation, and it behaves similarly electrophysiologically to *trans OK371/VGlut* combinations used in other studies (Daniels et al., 2004; Gaviño et al., 2015; Li et al., 2018).

There are differences between our study and the findings of other published work. Prior studies have used WT (or w^{1118}) as a control background when compared to VGlut overexpression (Daniels et al., 2004; Gaviño et al., 2015; Li et al., 2018). This is a standard practice. Those studies reported precise PHD when comparing WT vs. *OK371/VGlut* third instar larvae – decreased QC at *OK371/VGlut* NMJs resulting in unchanged evoked transmission. We replicated this finding (Fig. 1). However, we also used our Gal4 driver stock background *OK371/+* as an additional control. For that comparison, we saw a slight depression in the evoked amplitude of *OK371, VGlut/+* NMJs (Fig. 1). One possibility is that our recombinant stock was acting as a sensitized background to uncover conditions that might cause excess depression.

A second difference comes from the low extracellular calcium test. A low extracellular calcium experiment was previously done when VGlut overexpression was first characterized (Daniels et al., 2004). For that study, the authors showed that QC was significantly diminished compared to wild-type NMJs by the method of failure analysis. Taking the data of that study in aggregate, the authors concluded that PHD was intact in a variety of conditions, including saline with very low extracellular [Ca^{2+}] (0.23 mM Ca^{2+}, 20 mM Mg^{2+}). Our study may appear to conflict with that study because we found that saline with very low [Ca^{2+}] (0.2 mM Ca^{2+}, 10mM Mg^{2+}) is conducive to "excess PHD." One possibility is that since the original study was examining failure percentage vs. WT – and not the absolute value of mEPSPs or EPSPs in low calcium – a finding like excess depression might not be as easily observed. Other differences might be attributed genetic background or other differences in recording saline, like magnesium concentration.

Finally, one other study previously examined the effects of a cac^S mutation with concomitant VGlut overexpression (Gaviño et al., 2015). The authors did not find the low evoked potentials that we report. The major difference between that experiment and ours is that the prior work examined the cac^S mutation in an extracellular [Ca^{2+}] (1.0 mM) that was double that of our study. The result was a Ca^{2+} driving force that yielded robust baseline EPSPs, even in the cac^S mutant background (Gaviño et al., 2015). Given our results with calcium concentration (Fig. 6), a similar effect may work to resolve any sort of tuning problem with PHD compensation that we uncovered here.

How do calcium stores tune PHD?

How exactly might calcium stores impact PHD tuning? Less is understood about this. We know that endoplasmic reticulum (ER) can be visualized at Drosophila NMJ terminals (Summerville et al., 2016), and recently developed imaging tools can show how nerve stimulation results in dynamic changes to ER lumenal calcium, including at the Drosophila NMJ (de Juan-Sanz et al., 2017; Handler et al., 2019; Oliva et al., 2020). In parallel, other groups working at the NMJ have demonstrated important roles in baseline neurotransmission and in PHP for ER resident proteins (Genç et al., 2017; Kikuma et al., 2017). And from our prior work at the NMJ, we know that store calcium channels and upstream signaling components are important for maintaining the NMJ's capacity for PHP throughout life (Brusich et al., 2015; James et al., 2019). We also know that disrupting these same factors can ameliorate hyperexcitability associated with gains of Ca_V2 function (Brusich et al., 2018). Finally, from mammalian work it is clear that IP_3Rs, RyRs, and intracellular calcium govern a variety of forms of neuroplasticity (Berridge, 2016), including paired pulse facilitation (Emptage et al., 2001), and modulation of voltage-gated calcium channel activity (Catterall, 2011; Lee et al., 2000).

If PHD were simply a matter of properly functioning neurotransmission machinery, then it is not entirely obvious why PHD would be so sensitive to the amount calcium available such that its tuning point would become disoriented, either when store-operated channels were impaired or when the amount of influx was lowered. In our study, neurotransmission has not been lowered beyond a point of synapse failure. This means that there is still functional machinery. And PHD, per se, is not disrupted – indeed, there is still depression. With any type of homeostatic system, there not only needs to be error detection (large quantal size) and correction (decreased quantal content), but there also need to be brakes applied to the system to prevent some kind of overcorrection. Our data suggest some manner of PHD "overcorrection." In our view, this is an interesting and understudied type of phenomenon that could be examined in other homeostatic systems as well.

So how exactly do levels of calcium (or the function of distinct types of calcium channels found at the synapse) ultimately affect PHD correction levels? This is a difficult problem. The first step might be to narrow the relevant tissue type(s) involved in PHD signaling. ER and store-operated channels are relevant to the functions of many tissues. In principle, our genetic loss-of-function manipulations to *itpr* and *RyR* could affect store-operated channels either in the neuron or in the muscle or in surrounding tissues like glia. Our pharmacological manipulations using Dantrolene and Xestospongin C could also affect multiple tissue types. Therefore, in principle, changing the levels of cytosolic calcium could either affect local signaling in the neuron, or it could result in aberrant signaling back to the presynaptic neuron, disorienting the homeostat.

We favor the idea that the relevant calcium signal is local in the motor neuron for two reasons. First, from our own data, we were able to observe the excess depression (or overcorrection) phenotype either with manipulations to store calcium or with manipulations that affect presynaptic calcium influx, including partial loss-of-function of neuronal *cacophony*. Second, a recent study puts forth data suggesting that when VGlut overexpression induces PHD, this happens exclusively because of excess presynaptic glutamate release, and presynaptic depression is initiated independent of any sort of postsynaptic response (Li et al., 2018). Such an autocrine signaling mechanism could very well reveal a role for intracellular calcium signaling in the presynapse.

5 References

Berridge, M.J. (1984). Inositol trisphosphate and diacylglycerol as second messengers. Biochem J *220*, 345-360.

Berridge, M.J. (1987). Inositol trisphosphate and diacylglycerol: two interacting second messengers. Annu Rev Biochem *56*, 159-193.

Berridge, M.J. (1998). Neuronal calcium signaling. Neuron *21*, 13-26.

Berridge, M.J. (2016). The Inositol Trisphosphate/Calcium Signaling Pathway in Health and Disease. Physiol Rev *96*, 1261-1296.

Böhme, M.A., McCarthy, A.W., Grasskamp, A.T., Beuschel, C.B., Goel, P., Jusyte, M., Laber, D., Huang, S., Rey, U., Petzoldt, A.G., *et al.* (2019). Rapid active zone remodeling consolidates presynaptic potentiation. Nat Commun *10*, 1085.

Brusich, D.J., Spring, A.M., and Frank, C.A. (2015). A single-cross, RNA interference-based genetic tool for examining the long-term maintenance of homeostatic plasticity. Frontiers in cellular neuroscience *9*, 107.

451 Brusich, D.J., Spring, A.M., James, T.D., Yeates, C.J., Helms, T.H., and Frank, C.A. (2018).
452 Drosophila CaV2 channels harboring human migraine mutations cause synapse hyperexcitability that
453 can be suppressed by inhibition of a Ca2+ store release pathway. PLoS genetics *14*, e1007577.

454 Catterall, W.A. (2011). Voltage-gated calcium channels. Cold Spring Harbor perspectives in biology
455 *3*, a003947.

456 Cull-Candy, S.G., Miledi, R., Trautmann, A., and Uchitel, O.D. (1980). On the release of transmitter
457 at normal, myasthenia gravis and myasthenic syndrome affected human end-plates. J Physiol *299*, 621-
458 638.

459 Daniels, R.W., Collins, C.A., Gelfand, M.V., Dant, J., Brooks, E.S., Krantz, D.E., and DiAntonio, A.
460 (2004). Increased expression of the Drosophila vesicular glutamate transporter leads to excess
461 glutamate release and a compensatory decrease in quantal content. J Neurosci *24*, 10466-10474.

462 Davis, G.W. (2013). Homeostatic signaling and the stabilization of neural function. Neuron *80*, 718-
463 728.

464 Davis, G.W., DiAntonio, A., Petersen, S.A., and Goodman, C.S. (1998). Postsynaptic PKA controls
465 quantal size and reveals a retrograde signal that regulates presynaptic transmitter release in Drosophila.
466 Neuron *20*, 305-315.

467 Davis, G.W., and Müller, M. (2015). Homeostatic control of presynaptic neurotransmitter release.
468 Annu Rev Physiol *77*, 251-270.

469 de Juan-Sanz, J., Holt, G.T., Schreiter, E.R., de Juan, F., Kim, D.S., and Ryan, T.A. (2017). Axonal
470 Endoplasmic Reticulum Ca(2+) Content Controls Release Probability in CNS Nerve Terminals.
471 Neuron *93*, 867-881 e866.

472 Delvendahl, I., and Müller, M. (2019). Homeostatic plasticity-a presynaptic perspective. Curr Opin
473 Neurobiol *54*, 155-162.

474 Dockendorff, T.C., Robertson, S.E., Faulkner, D.L., and Jongens, T.A. (2000). Genetic
475 characterization of the 44D-45B region of the Drosophila melanogaster genome based on an F2 lethal
476 screen. Molecular & general genetics : MGG *263*, 137-143.

477 Emptage, N.J., Reid, C.A., and Fine, A. (2001). Calcium stores in hippocampal synaptic boutons
478 mediate short-term plasticity, store-operated Ca2+ entry, and spontaneous transmitter release. Neuron
479 *29*, 197-208.

480 Frank, C.A. (2014a). Homeostatic plasticity at the Drosophila neuromuscular junction.
481 Neuropharmacology *78*, 63-74.

482 Frank, C.A. (2014b). How voltage-gated calcium channels gate forms of homeostatic synaptic
483 plasticity. Frontiers in cellular neuroscience *8*, 40.

484 Frank, C.A., James, T.D., and Muller, M. (2020). Homeostatic control of Drosophila neuromuscular
485 junction function. Synapse *74*, e22133.

486 Frank, C.A., Kennedy, M.J., Goold, C.P., Marek, K.W., and Davis, G.W. (2006). Mechanisms
487 underlying the rapid induction and sustained expression of synaptic homeostasis. Neuron *52*, 663-677.

488 Frank, C.A., Pielage, J., and Davis, G.W. (2009). A presynaptic homeostatic signaling system
489 composed of the Eph receptor, ephexin, Cdc42, and CaV2.1 calcium channels. Neuron *61*, 556-569.

490 Gafni, J., Munsch, J.A., Lam, T.H., Catlin, M.C., Costa, L.G., Molinski, T.F., and Pessah, I.N. (1997).
491 Xestospongins: potent membrane permeable blockers of the inositol 1,4,5-trisphosphate receptor.
492 Neuron *19*, 723-733.

493 Gaviño, M.A., Ford, K.J., Archila, S., and Davis, G.W. (2015). Homeostatic synaptic depression is
494 achieved through a regulated decrease in presynaptic calcium channel abundance. eLife *4*.

495 Genç, Ö., Dickman, D.K., Ma, W., Tong, A., Fetter, R.D., and Davis, G.W. (2017). MCTP is an ER-
496 resident calcium sensor that stabilizes synaptic transmission and homeostatic plasticity. eLife *6*.

497 Goel, P., Dufour Bergeron, D., Bohme, M.A., Nunnelly, L., Lehmann, M., Buser, C., Walter, A.M.,
498 Sigrist, S.J., and Dickman, D. (2019). Homeostatic scaling of active zone scaffolds maintains global
499 synaptic strength. J Cell Biol *218*, 1706-1724.

500 Gratz, S.J., Goel, P., Bruckner, J.J., Hernandez, R.X., Khateeb, K., Macleod, G.T., Dickman, D., and
501 O'Connor-Giles, K.M. (2019). Endogenous Tagging Reveals Differential Regulation of Ca(2+)
502 Channels at Single Active Zones during Presynaptic Homeostatic Potentiation and Depression. J
503 Neurosci *39*, 2416-2429.

504 Handler, A., Graham, T.G.W., Cohn, R., Morantte, I., Siliciano, A.F., Zeng, J., Li, Y., and Ruta, V.
505 (2019). Distinct Dopamine Receptor Pathways Underlie the Temporal Sensitivity of Associative
506 Learning. Cell *178*, 60-75 e19.

507 Hazelrigg, T., Levis, R., and Rubin, G.M. (1984). Transformation of white locus DNA in drosophila:
508 dosage compensation, zeste interaction, and position effects. Cell *36*, 469-481.

509 James, T.D., Zwiefelhofer, D.J., and Frank, C.A. (2019). Maintenance of homeostatic plasticity at the
510 Drosophila neuromuscular synapse requires continuous IP3-directed signaling. eLife *8*.

511 Jeans, A.F., van Heusden, F.C., Al-Mubarak, B., Padamsey, Z., and Emptage, N.J. (2017). Homeostatic
512 Presynaptic Plasticity Is Specifically Regulated by P/Q-type Ca(2+) Channels at Mammalian
513 Hippocampal Synapses. Cell reports *21*, 341-350.

514 Kawasaki, F., Collins, S.C., and Ordway, R.W. (2002). Synaptic calcium-channel function in
515 Drosophila: analysis and transformation rescue of temperature-sensitive paralytic and lethal mutations
516 of cacophony. J Neurosci *22*, 5856-5864.

517 Kawasaki, F., Felling, R., and Ordway, R.W. (2000). A temperature-sensitive paralytic mutant defines
518 a primary synaptic calcium channel in Drosophila. J Neurosci *20*, 4885-4889.

519 Kawasaki, F., Zou, B., Xu, X., and Ordway, R.W. (2004). Active zone localization of presynaptic
520 calcium channels encoded by the cacophony locus of Drosophila. J Neurosci *24*, 282-285.

521 Kikuma, K., Li, X., Kim, D., Sutter, D., and Dickman, D.K. (2017). Extended Synaptotagmin Localizes
522 to Presynaptic ER and Promotes Neurotransmission and Synaptic Growth in Drosophila. Genetics *207*,
523 993-1006.

524 Lee, A., Scheuer, T., and Catterall, W.A. (2000). Ca2+/calmodulin-dependent facilitation and
525 inactivation of P/Q-type Ca2+ channels. J Neurosci *20*, 6830-6838.

526 Lefebvre, S., Burglen, L., Reboullet, S., Clermont, O., Burlet, P., Viollet, L., Benichou, B., Cruaud,
527 C., Millasseau, P., Zeviani, M., *et al.* (1995). Identification and characterization of a spinal muscular
528 atrophy-determining gene. Cell *80*, 155-165.

529 Li, X., Goel, P., Wondolowski, J., Paluch, J., and Dickman, D. (2018). A Glutamate Homeostat
530 Controls the Presynaptic Inhibition of Neurotransmitter Release. Cell reports *23*, 1716-1727.

531 Mahr, A., and Aberle, H. (2006). The expression pattern of the Drosophila vesicular glutamate
532 transporter: a marker protein for motoneurons and glutamatergic centers in the brain. Gene expression
533 patterns : GEP *6*, 299-309.

534 Marder, E., and Goaillard, J.M. (2006). Variability, compensation and homeostasis in neuron and
535 network function. Nat Rev Neurosci *7*, 563-574.

536 Marie, B., Pym, E., Bergquist, S., and Davis, G.W. (2010). Synaptic homeostasis is consolidated by
537 the cell fate gene gooseberry, a Drosophila pax3/7 homolog. J Neurosci *30*, 8071-8082.

538 Martin, A.R. (1955). A further study of the statistical composition on the end-plate potential. J Physiol
539 *130*, 114-122.

540 Meyer, F., and Aberle, H. (2006). At the next stop sign turn right: the metalloprotease Tolloid-related
541 1 controls defasciculation of motor axons in Drosophila. Development *133*, 4035-4044.

542 Müller, M., and Davis, G.W. (2012). Transsynaptic control of presynaptic Ca(2)(+) influx achieves
543 homeostatic potentiation of neurotransmitter release. Curr Biol *22*, 1102-1108.

544 Oliva, M.K., Perez-Moreno, J.J., O'Shaughnessy, J., Wardill, T.J., and O'Kane, C.J. (2020).
545 Endoplasmic Reticulum Lumenal Indicators in Drosophila Reveal Effects of HSP-Related Mutations
546 on Endoplasmic Reticulum Calcium Dynamics. Front Neurosci *14*, 816.

547 Petersen, S.A., Fetter, R.D., Noordermeer, J.N., Goodman, C.S., and DiAntonio, A. (1997). Genetic
548 analysis of glutamate receptors in Drosophila reveals a retrograde signal regulating presynaptic
549 transmitter release. Neuron *19*, 1237-1248.

550 Pozo, K., and Goda, Y. (2010). Unraveling mechanisms of homeostatic synaptic plasticity. Neuron *66*,
551 337-351.

552 Raimer, A.C., Singh, S.S., Edula, M.R., Paris-Davila, T., Vandadi, V., Spring, A.M., and Matera, A.G.
553 (2020). Temperature-sensitive spinal muscular atrophy-causing point mutations lead to SMN
554 instability, locomotor defects and premature lethality in Drosophila. Dis Model Mech *13*.

555 Sen, A., Yokokura, T., Kankel, M.W., Dimlich, D.N., Manent, J., Sanyal, S., and Artavanis-Tsakonas,
556 S. (2011). Modeling spinal muscular atrophy in Drosophila links Smn to FGF signaling. J Cell Biol
557 *192*, 481-495.

558 Simkus, C.R., and Stricker, C. (2002). The contribution of intracellular calcium stores to mEPSCs
559 recorded in layer II neurones of rat barrel cortex. J Physiol *545*, 521-535.

560 Smith, L.A., Peixoto, A.A., Kramer, E.M., Villella, A., and Hall, J.C. (1998). Courtship and visual
561 defects of cacophony mutants reveal functional complexity of a calcium-channel alpha1 subunit in
562 Drosophila. Genetics *149*, 1407-1426.

563 Spring, A.M., Brusich, D.J., and Frank, C.A. (2016). C-terminal Src Kinase Gates Homeostatic
564 Synaptic Plasticity and Regulates Fasciclin II Expression at the Drosophila Neuromuscular Junction.
565 PLoS genetics *12*, e1005886.

566 Spring, A.M., Raimer, A.C., Hamilton, C.D., Schillinger, M.J., and Matera, A.G. (2019).
567 Comprehensive Modeling of Spinal Muscular Atrophy in Drosophila melanogaster. Frontiers in
568 molecular neuroscience *12*, 113.

569 Summerville, J.B., Faust, J.F., Fan, E., Pendin, D., Daga, A., Formella, J., Stern, M., and McNew, J.A.
570 (2016). The effects of ER morphology on synaptic structure and function in Drosophila melanogaster.
571 Journal of cell science *129*, 1635-1648.

572 Turrigiano, G.G. (2008). The self-tuning neuron: synaptic scaling of excitatory synapses. Cell *135*,
573 422-435.

574 Vazquez-Martinez, O., Canedo-Merino, R., Diaz-Munoz, M., and Riesgo-Escovar, J.R. (2003).
575 Biochemical characterization, distribution and phylogenetic analysis of Drosophila melanogaster

ryanodine and IP3 receptors, and thapsigargin-sensitive Ca2+ ATPase. Journal of cell science *116*, 2483-2494.

Venkatesh, K., and Hasan, G. (1997). Disruption of the IP3 receptor gene of Drosophila affects larval metamorphosis and ecdysone release. Curr Biol *7*, 500-509.

Wang, X., Pinter, M.J., and Rich, M.M. (2016). Reversible Recruitment of a Homeostatic Reserve Pool of Synaptic Vesicles Underlies Rapid Homeostatic Plasticity of Quantal Content. J Neurosci *36*, 828-836.

Wilcox, R.A., Primrose, W.U., Nahorski, S.R., and Challiss, R.A. (1998). New developments in the molecular pharmacology of the myo-inositol 1,4,5-trisphosphate receptor. Trends Pharmacol Sci *19*, 467-475.

Yeates, C.J., Zwiefelhofer, D.J., and Frank, C.A. (2017). The Maintenance of Synaptic Homeostasis at the Drosophila Neuromuscular Junction Is Reversible and Sensitive to High Temperature. eNeuro *4*.

Zhao, C., Dreosti, E., and Lagnado, L. (2011). Homeostatic synaptic plasticity through changes in presynaptic calcium influx. J Neurosci *31*, 7492-7496.

Zhao, F., Li, P., Chen, S.R., Louis, C.F., and Fruen, B.R. (2001). Dantrolene inhibition of ryanodine receptor Ca2+ release channels. Molecular mechanism and isoform selectivity. J Biol Chem *276*, 13810-13816.

6 Figure Legends

Figure 1. Presynaptic homeostatic depression (PHD) works successfully with a recombinant line of *OK371-Gal4* and *UAS-VGlut*. (A) NMJ electrophysiological data for miniature excitatory postsynaptic potentials (mEPSP), excitatory postsynaptic potentials (EPSP), and quantal content (QC). Data are normalized to WT (w^{1118}) values. *VGlut, OK371/+* NMJs have increased mEPSP but normal EPSP because of decreased QC, indicative of successful PHD. (*** $p < 0.001$ vs. WT by one-way ANOVA with Tukey's post-hoc). **(B)** Representative electrophysiological traces. Large traces are EPSPs; small traces are mEPSPs. Scale bars for EPSPs (mEPSPs) are 5 mV (1 mV) and 50 ms (1000 ms). **(C)** Raw data for mEPSPs. **(D)** Raw data for EPSPs. **(E)** Raw data for QC. For (C)-(E), bars are averages and error bars are ± SEM. *** $p < 0.001$ vs. WT or vs. *OK371/+*; # $p < 0.05$ vs. *OK371/+*; analyses by one-way ANOVA with Tukey's post-hoc.

Figure 2. A screen to uncover conditions with defective PHD. (A) Crossing scheme for generating larvae for electrophysiological recording. Each animal recorded had a homeostatic challenge provided by VGlut overexpression and a concurrent heterozygous or RNAi condition. **(B)** Data distribution for screened conditions (x-axis = average EPSP for condition; y-axis = average QC for condition). Green = *UAS-VGlut, OK371-Gal4/+*. Red = *UAS-VGlut, OK371-Gal4/RyRE4340K; itpr90B/+*. Purple = *UAS-VGlut, OK371-Gal4/+; UAS-Smn[RNAi]^{JF02057}/+*. Dotted line: EPSP value two standard deviations below *UAS-VGlut, OK371-Gal4/+* chosen as a cut off for potential follow-up hits. **(C)** Average EPSPs for screened conditions. All conditions have a *UAS-VGlut, OK371-Gal4/+* genetic background. ">" denotes as *UAS* construct or RNAi line being driven in motor neurons by *OK371-Gal4*. "+" denotes additional mutations present as heterozygotes. Top dotted line denotes *UAS-VGlut, OK371-Gal4/+* average. Bottom dotted line denotes two standard deviations below *UAS-VGlut, OK371-Gal4/+* average.

Figure 3. Double heterozygous loss of the *itpr* and *RyR* genes causes excess depression. Note: Traces and data for *OK371/+* and *VGlut, OK371/+* are repeated from Figure 1 for comparison purposes. Abbreviations are as in Figure 1 as well. **(A)** NMJ electrophysiological data for mEPSP, EPSP, and QC. Data are normalized to *OK371/+* values. * $p < 0.05$, ** $p < 0.01$, and *** $p < 0.001$ vs. *OK371/+*; ## $p < 0.01$ and ### $p < 0.001$ vs. *OK371/RyRE4340K; itpr90B/+*; analyses by one-way ANOVA with Tukey's post-hoc. **(B)** Raw data for mEPSPs. **(C)** Raw data for EPSPs. **(D)** Raw data for QC. For (B)-(D), bars are averages and error bars are ± SEM. * $p < 0.05$, ** $p < 0.01$, and *** $p < 0.001$ by one-way ANOVA with Tukey's post-hoc. **(E)** Representative electrophysiological traces with S.D. and range values for EPSPs shown. The evoked amplitude S.D. and range were significantly higher for *VGlut, OK371/RyR^{E4340K}; itpr^{90B}/+* vs. its genetic control, *OK371/RyR^{E4340K}; itpr^{90B}/+*. * $p < 0.05$, ** $p < 0.01$ by one-way ANOVA with Tukey's post-hoc. Scale bars as in Figure 1.

Figure 4. Genetic impairment of *itpr* combined with pharmacological impairment of RyR causes excess depression. (A) Raw data for mEPSPs (left); raw data for EPSPs (middle); raw data for QC (right). All data are for the indicated NMJ genotypes with 25 µM Dantrolene; bars are averages and error bars are ± SEM. * $p < 0.05$, ** $p < 0.01$, and *** $p < 0.001$ by one-way ANOVA with Tukey's post-hoc. **(B)** Representative EPSP traces. Scale bars are as in Figure 1.

Figure 5. Additional pharmaco-genetic combinations cause excess depression. (A) Raw data for mEPSPs (left); raw data for EPSPs (middle); raw data for QC (right). All data are for the indicated NMJ genotypes with 25 µM Dantrolene; bars are averages and error bars are ± SEM. **(B)** Data as in (A) but with 20 µM Xestospongin C instead of Dantrolene. **(C)** Representative EPSP traces. Scale bars are as in Figure 1. * $p < 0.05$, ** $p < 0.01$, and *** $p < 0.001$ by Student's T-Test comparing a control dataset (no VGlut overexpression) vs. an experimental dataset (VGlut overexpression).

Figure 6. Ca^{2+} concentration-sensitivity of PHD execution. (A) Log-log plots of recording saline [Ca^{2+}] vs. QC corrected for non-linear summation for WT, *OK371/+*, and *VGlut, OK371/+* conditions. Across the range of [Ca^{2+}] examined, there is no significant difference in calcium cooperativity for these conditions (Nonlinear Regression, $p = 0.91$). **(B)** Data plotted as in (A) but this time with a double heterozygous *RyR^{E4340K}/+; itpr^{90B}/+* genetic background. Across the range of [Ca^{2+}] examined, there is no significant difference in calcium cooperativity for these conditions (Nonlinear Regression, $p = 0.78$). **(C)** Raw data for mEPSPs (left); raw data for EPSPs (middle); raw data for QC (right). All data are for the indicated NMJ genotypes in 0.2 mM [Ca^{2+}]; bars are averages and error bars are ± SEM. For mEPSPs, * $p < 0.05$ and *** $p < 0.001$ by Student's T-Test, comparing PHD-challenged genotypes vs. unchallenged genetic controls. For EPSPs and QC, * $p < 0.05$, ** $p < 0.01$, and *** $p < 0.001$ vs. *OK371/+*; ## $p < 0.01$; EPSP and QC analyses done across multiple genotypes by one-way ANOVA with Tukey's post-hoc.

Figure 7. Partial impairment of Ca_V2/Cacophony causes excess depression. (A) Crossing scheme for generating larvae for electrophysiological recording. Male larvae were hemizygous for the *cac^S* hypomorphic mutation. **(B)** Raw data for mEPSPs. **(C)** Raw data for EPSPs. **(D)** Raw data for QC. For (B)-(D), bars are averages and error bars are ± SEM. * $p < 0.05$, ** $p < 0.01$, and *** $p < 0.001$ by Student's T-Test comparing the control *cac^S* dataset (no *VGlut* overexpression) vs. the experimental cac^S dataset (*VGlut* overexpression).

Figure 8. Model for how multiple calcium sources tune the process of PHD. Under baseline conditions, Ca_V2-type calcium channels contribute to synapse function, as may RyRs and IP_3Rs. Under conditions inducing PHD, synaptic vesicles are enlarged, and QC is decreased, possibly through

regulation of sources of calcium. When PHD challenge is coupled with concomitant impairment of RyR and IP_3R channels, evoked potentials are significantly diminished, due to excess PHD.

7 Conflict of Interest

The authors declare that the research was conducted in the absence of any commercial or financial relationships that could be construed as a potential conflict of interest.

8 Author Contributions

C.J.Y. and C.A.F. both did the following: designed research, performed research, analysed data, and wrote and edited the paper.

9 Funding

Funding supporting this work includes an NSF Grant (1557792) and an NIH/NINDS Grant (R01NS085164) to C.A.F. C.J.Y. was supported in part by an NIH/NINDS Predoctoral Training Grant to the University of Iowa (UI) Interdisciplinary Graduate Program in Neuroscience (T32NS007421 – PI Daniel T. Tranel), as well as a post-comprehensive exam predoctoral summer fellowship and a Ballard and Seashore Dissertation fellowship via the Graduate College at UI.

10 Acknowledgments

We thank members of the Frank lab for helpful comments. We thank the laboratories of Drs. Tina Tootle, Fang Lin, Toshihiro Kitamoto, Pamela Geyer, and Lori Wallrath for helpful discussions. We also thank Drs. Toshihiro Kitamoto, Joshua Weiner, Christopher Stipp, and Mark Stamnes for helpful feedback on an earlier written version of this study.

11 Supplementary Material

Please see Supplementary Table S1 for raw data from the electrophysiology screen and a legend explaining the table.

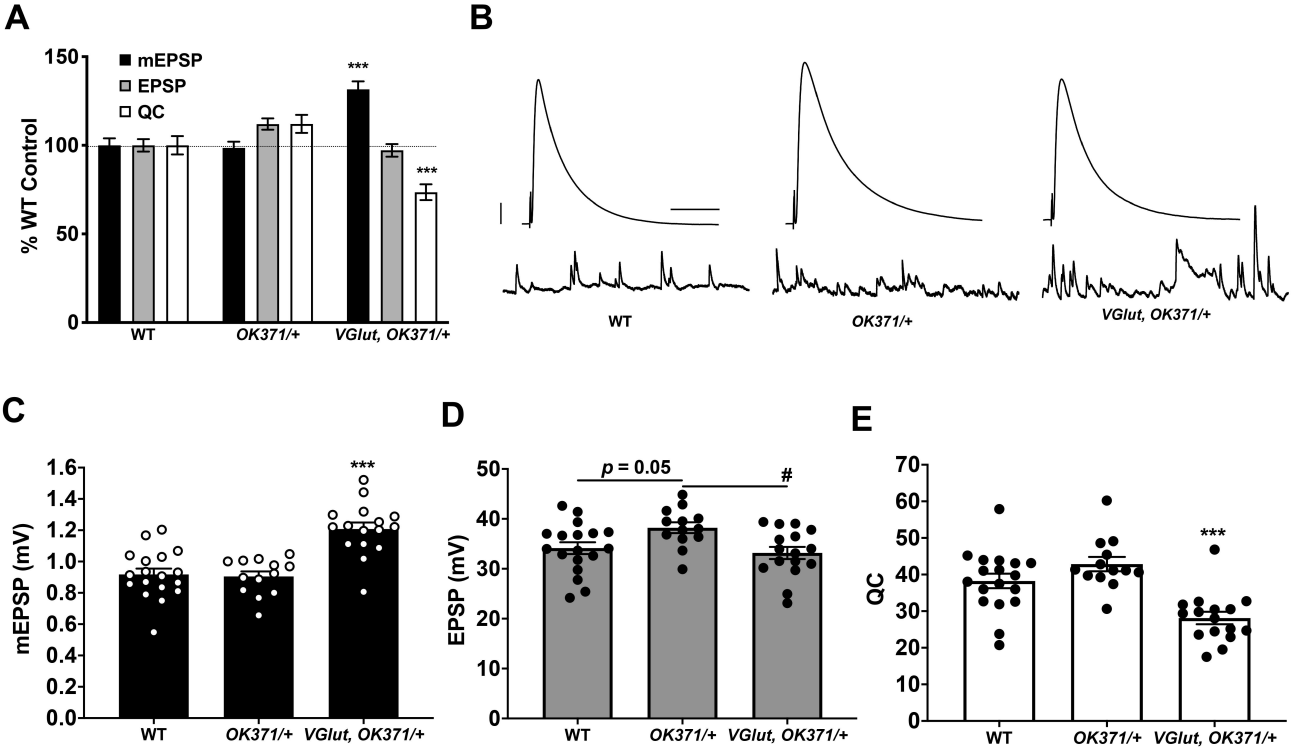
A
150
100
50
0
% WT Control
mEPSP
EPSP
QC
***
***
WT
OK371/+
VGlut, OK371/+
B
WT
OK371/+
VGlut, OK371/+
C
1.6
1.4
1.2
1.0
0.8
0.6
0.4
0.2
0.0
mEPSP (mV)
***
WT
OK371/+
VGlut, OK371/+
D
50
40
30
20
10
0
EPSP (mV)
p = 0.05
#
WT
OK371/+
VGlut, OK371/+
E
70
60
50
40
30
20
10
0
QC
***
WT
OK371/+
VGlut, OK371/+

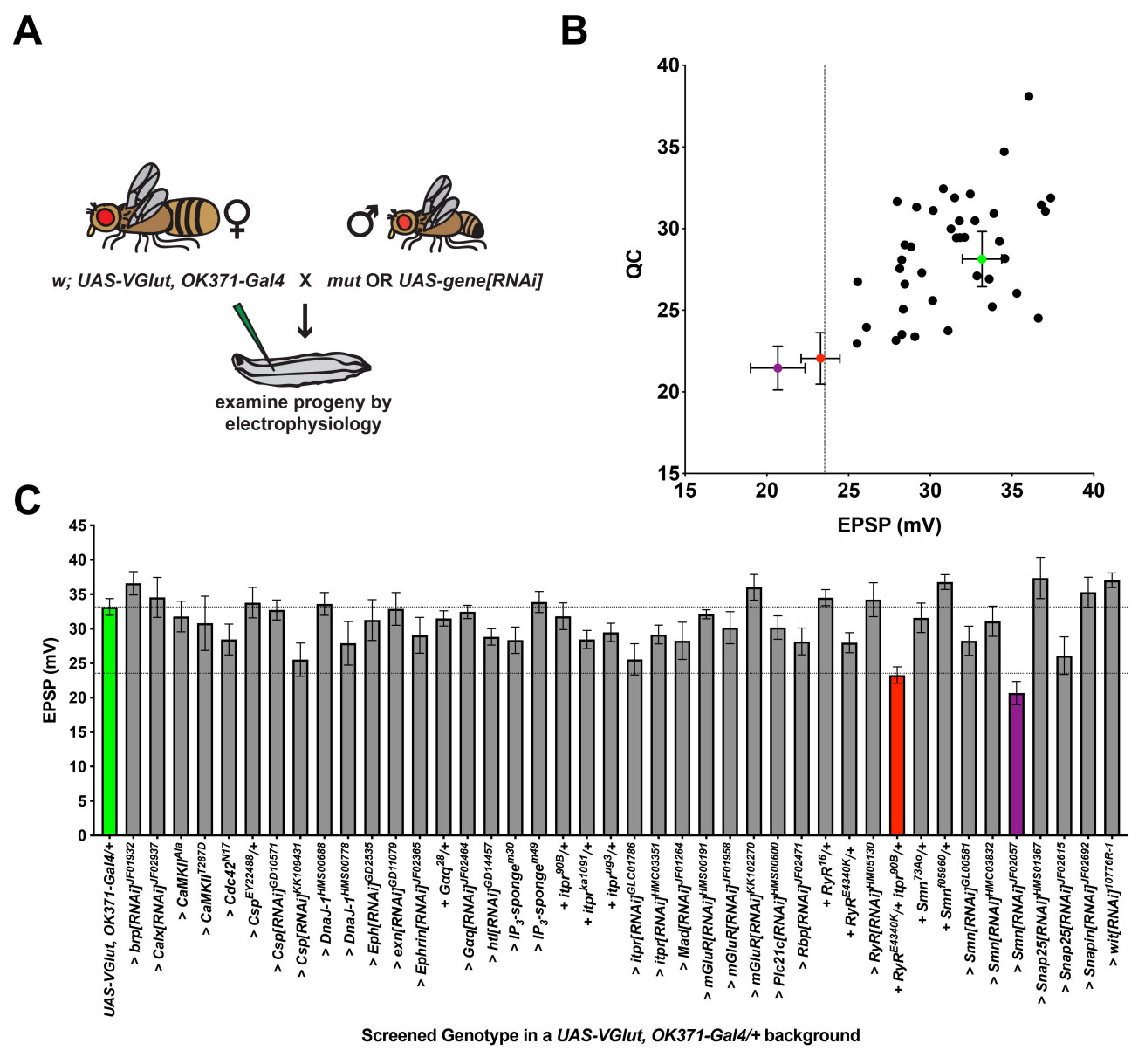
A
w; UAS-VGlut, OK371-Gal4 X mut OR UAS-gene[RNAi]
examine progeny by electrophysiology
B
QC
EPSP (mV)
C
EPSP (mV)
UAS-VGlut, OK371-Gal4/+
> brp[RNAi]JF01932
> Calx[RNAi]JF02937
> CaMKII^Ala
> CaMKII^T287D
> Cdc42^N17
> Csp^EY22488/+
> Csp[RNAi]GD10571
> Csp[RNAi]KK109431
> DnaJ-1[RNAi]HMS00688
> DnaJ-1[RNAi]HMS00778
> Eph[RNAi]GD2535
> exn[RNAi]GD11079
> Ephrin[RNAi]JF02365
+ Gaq^28/+
> Gaq[RNAi]JF02464
> htl[RNAi]GD14457
> IP3-sponge^m30
> IP3-sponge^m49
+ itpr^90B/+
+ itpr^ka1091/+
+ itpr^ug3/+
> itpr[RNAi]GLC01786
> itpr[RNAi]HMC03351
> Mad[RNAi]JF01264
> mGluR[RNAi]HMS00191
> mGluR[RNAi]JF01958
> mGluR[RNAi]KK102270
> Plc21c[RNAi]HMS00600
> Rbp[RNAi]JF02471
+ RyR^16/+
+ RyR^E4340K/+
> RyR[RNAi]HM05130
+ RyR^E4340K/+ itpr^90B/+
+ Smn^73Ao/+
+ Smn^f05960/+
> Smn[RNAi]GL00581
> Smn[RNAi]HMC03832
> Smn[RNAi]JF02057
> Snap25[RNAi]HMS01367
> Snap25[RNAi]JF02615
> Snapin[RNAi]JF02692
> wit[RNAi]10776R-1
Screened Genotype in a UAS-VGlut, OK371-Gal4/+ background

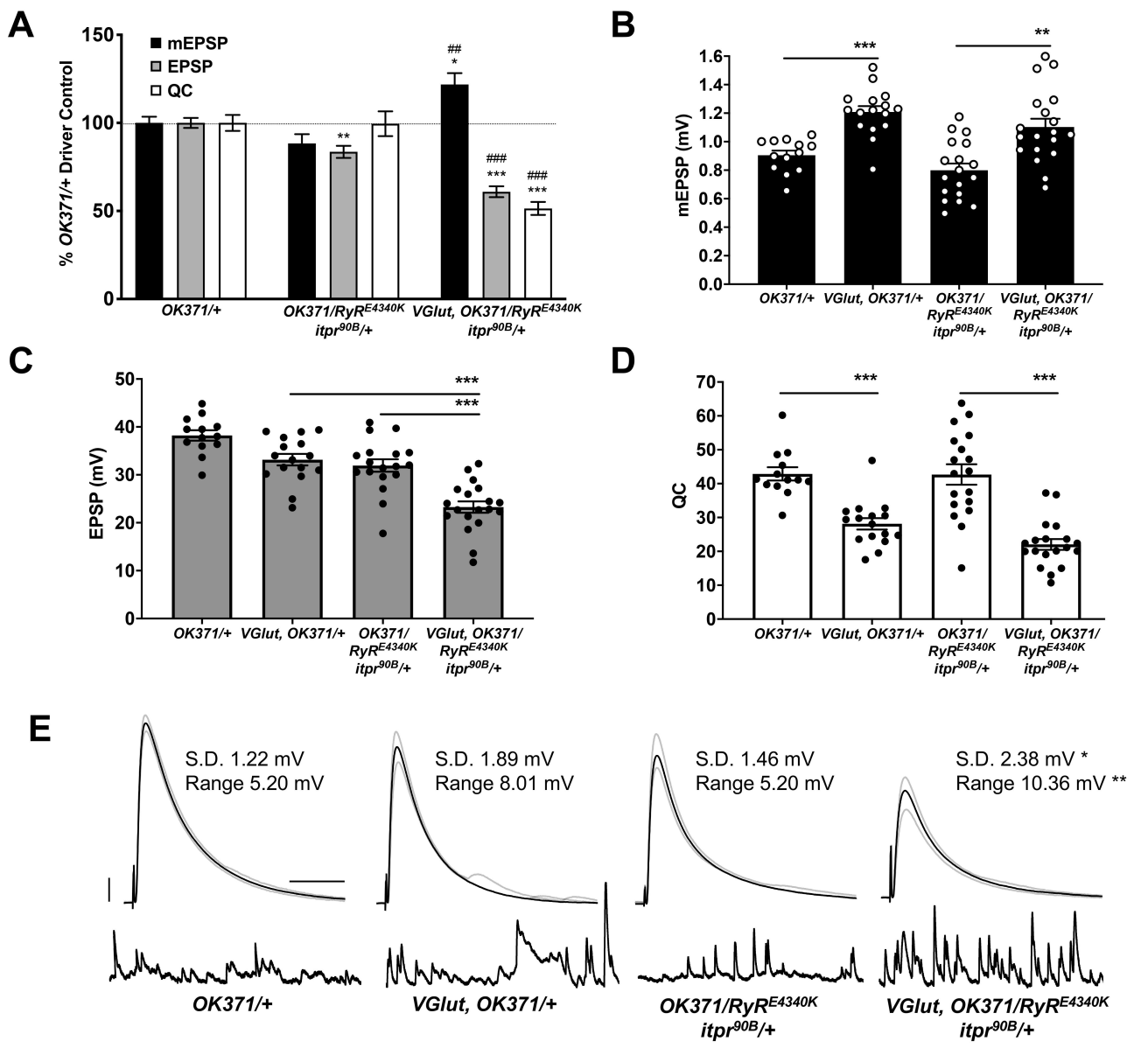
A
mEPSP
EPSP
QC
% OK371/+ Driver Control
150
100
50
0
##
*
**
###
***
###
***
OK371/+
OK371/RyR^{E4340K} itpr^{90B}/+
VGlut, OK371/RyR^{E4340K} itpr^{90B}/+
B
mEPSP (mV)
1.6
1.4
1.2
1.0
0.8
0.6
0.4
0.2
0.0
***
**
OK371/+
VGlut, OK371/+
OK371/ RyR^{E4340K} itpr^{90B}/+
VGlut, OK371/ RyR^{E4340K} itpr^{90B}/+
C
EPSP (mV)
50
40
30
20
10
0
***
***
OK371/+
VGlut, OK371/+
OK371/ RyR^{E4340K} itpr^{90B}/+
VGlut, OK371/ RyR^{E4340K} itpr^{90B}/+
D
QC
70
60
50
40
30
20
10
0
***
***
OK371/+
VGlut, OK371/+
OK371/ RyR^{E4340K} itpr^{90B}/+
VGlut, OK371/ RyR^{E4340K} itpr^{90B}/+
E
S.D. 1.22 mV
Range 5.20 mV
S.D. 1.89 mV
Range 8.01 mV
S.D. 1.46 mV
Range 5.20 mV
S.D. 2.38 mV *
Range 10.36 mV **
OK371/+
VGlut, OK371/+
OK371/RyR^{E4340K} itpr^{90B}/+
VGlut, OK371/RyR^{E4340K} itpr^{90B}/+

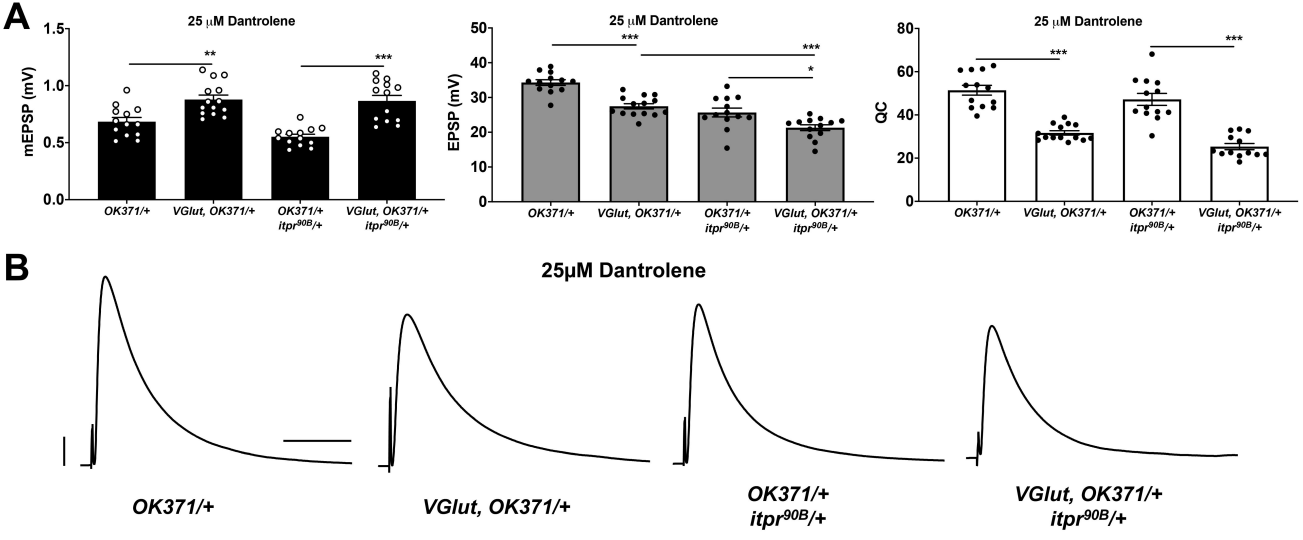
A
25 μM Dantrolene
mEPSP (mV)
1.5
1.0
0.5
0.0
**
***
OK371/+
VGlut, OK371/+
OK371/+ itpr90B/+
VGlut, OK371/+ itpr90B/+
25 μM Dantrolene
EPSP (mV)
50
40
30
20
10
0
***
***
*
OK371/+
VGlut, OK371/+
OK371/+ itpr90B/+
VGlut, OK371/+ itpr90B/+
25 μM Dantrolene
QC
80
60
40
20
0
***
***
OK371/+
VGlut, OK371/+
OK371/+ itpr90B/+
VGlut, OK371/+ itpr90B/+
B
25μM Dantrolene
OK371/+
VGlut, OK371/+
OK371/+ itpr90B/+
VGlut, OK371/+ itpr90B/+

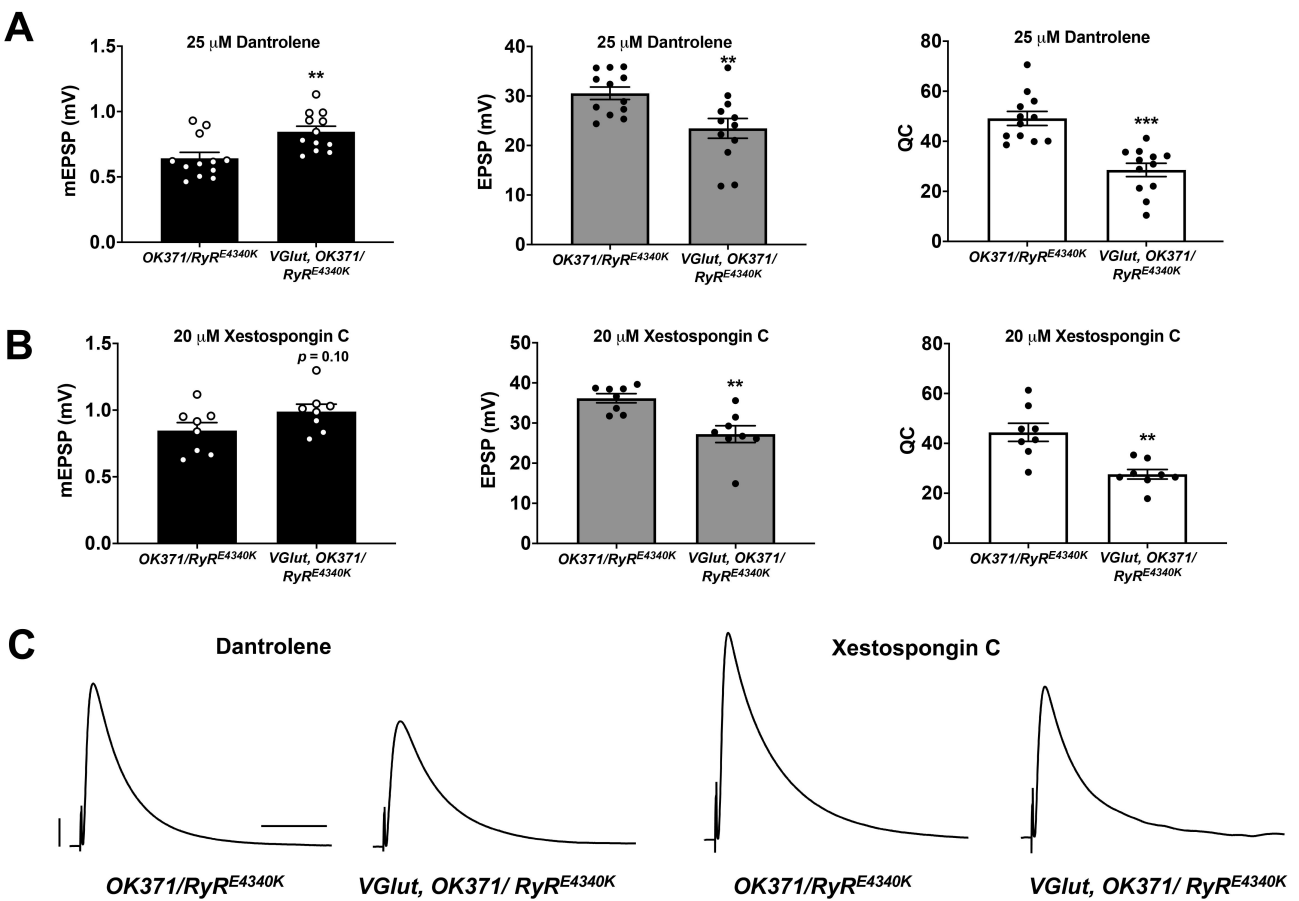
A
25 μM Dantrolene
mEPSP (mV)
1.5
1.0
0.5
0.0
**
OK371/RyR^{E4340K}
VGlut, OK371/ RyR^{E4340K}
25 μM Dantrolene
EPSP (mV)
40
30
20
10
0
**
OK371/RyR^{E4340K}
VGlut, OK371/ RyR^{E4340K}
25 μM Dantrolene
QC
80
60
40
20
0
***
OK371/RyR^{E4340K}
VGlut, OK371/ RyR^{E4340K}
B
20 μM Xestospongin C
mEPSP (mV)
1.5
1.0
0.5
0.0
p = 0.10
OK371/RyR^{E4340K}
VGlut, OK371/ RyR^{E4340K}
20 μM Xestospongin C
EPSP (mV)
50
40
30
20
10
0
**
OK371/RyR^{E4340K}
VGlut, OK371/ RyR^{E4340K}
20 μM Xestospongin C
QC
80
60
40
20
0
**
OK371/RyR^{E4340K}
VGlut, OK371/ RyR^{E4340K}
C
Dantrolene
Xestospongin C
OK371/RyR^{E4340K}
VGlut, OK371/ RyR^{E4340K}
OK371/RyR^{E4340K}
VGlut, OK371/ RyR^{E4340K}

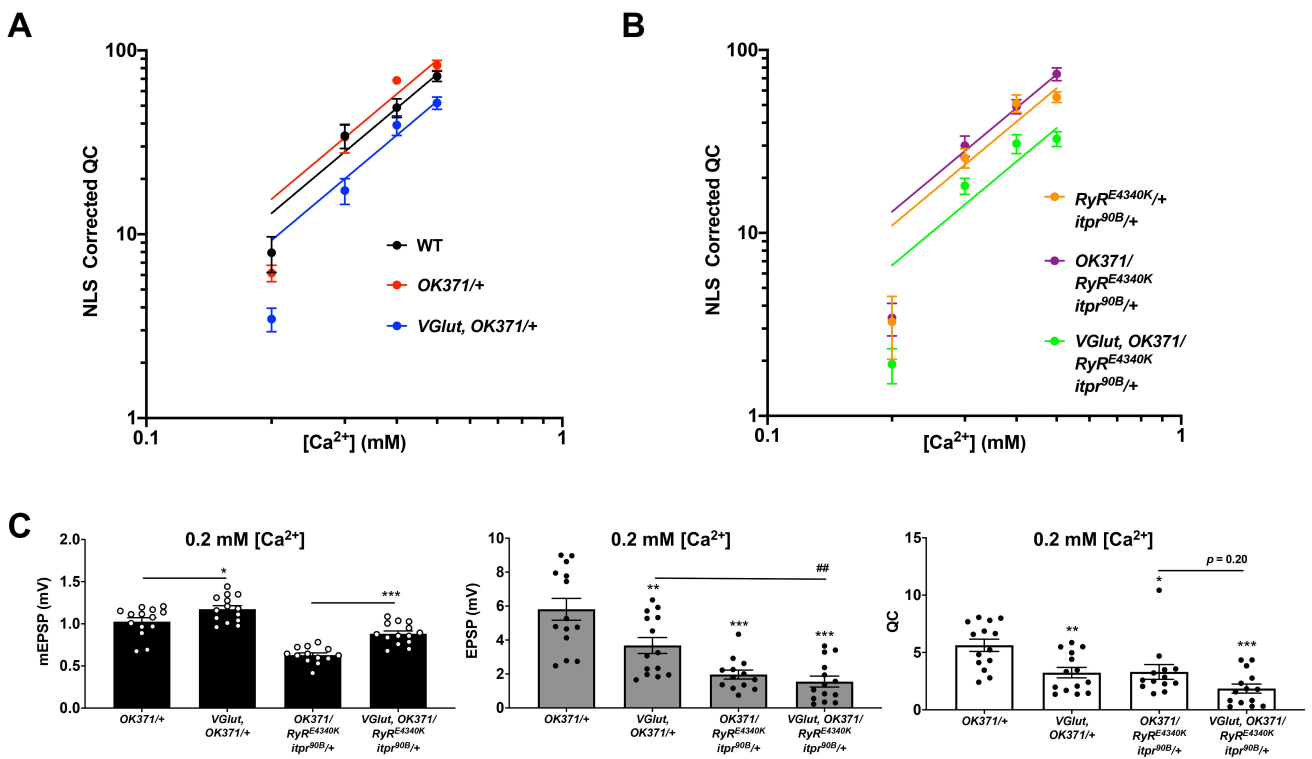
A
NLS Corrected QC
100
10
1
0.1
1
[Ca2+] (mM)
WT
OK371/+
VGlut, OK371/+
B
NLS Corrected QC
100
10
1
0.1
1
[Ca2+] (mM)
RyRE4340K/+
itpr90B/+
OK371/
RyRE4340K
itpr90B/+
VGlut, OK371/
RyRE4340K
itpr90B/+
C
0.2 mM [Ca2+]
mEPSP (mV)
2.0
1.5
1.0
0.5
0.0
*
***
OK371/+
VGlut, OK371/+
OK371/ RyRE4340K itpr90B/+
VGlut, OK371/ RyRE4340K itpr90B/+
0.2 mM [Ca2+]
EPSP (mV)
10
8
6
4
2
0
**
***
***
##
OK371/+
VGlut, OK371/+
OK371/ RyRE4340K itpr90B/+
VGlut, OK371/ RyRE4340K itpr90B/+
0.2 mM [Ca2+]
QC
15
10
5
0
p = 0.20
*
**
***
OK371/+
VGlut, OK371/+
OK371/ RyRE4340K itpr90B/+
VGlut, OK371/ RyRE4340K itpr90B/+

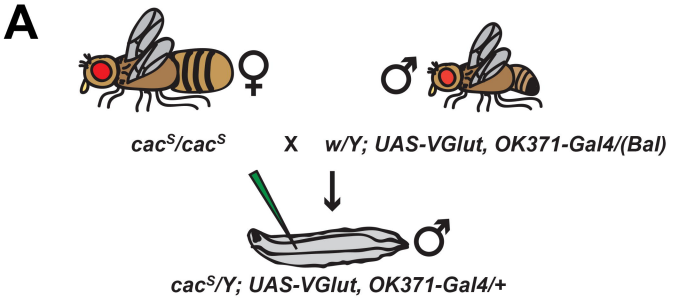
A
cacS/cacS
X
w/Y; UAS-VGlut, OK371-Gal4/(Bal)
cacS/Y; UAS-VGlut, OK371-Gal4/+

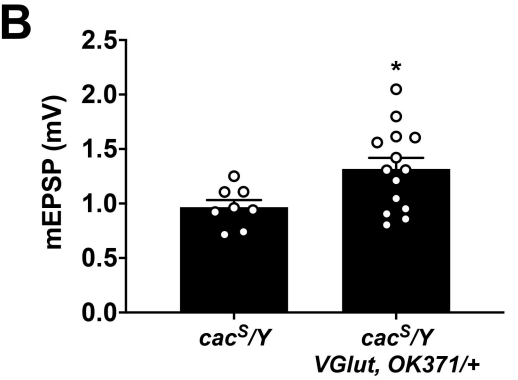
B
mEPSP (mV)
2.5
2.0
1.5
1.0
0.5
0.0
*
cacS/Y
cacS/Y
VGlut, OK371/+

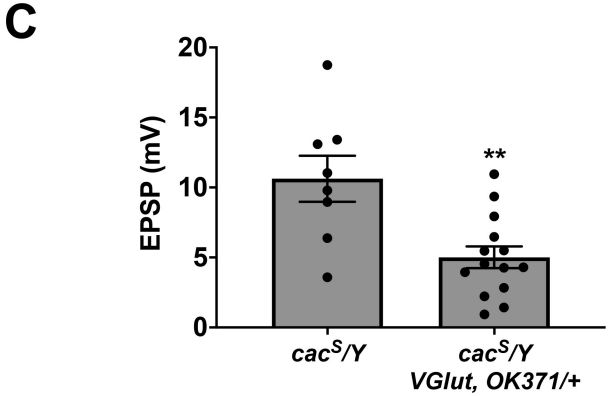
C
EPSP (mV)
20
15
10
5
0
**
cacS/Y
cacS/Y
VGlut, OK371/+

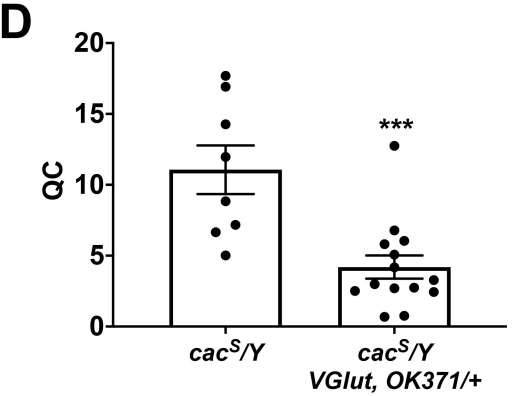
D
QC
20
15
10
5
0
***
cacS/Y
cacS/Y
VGlut, OK371/+

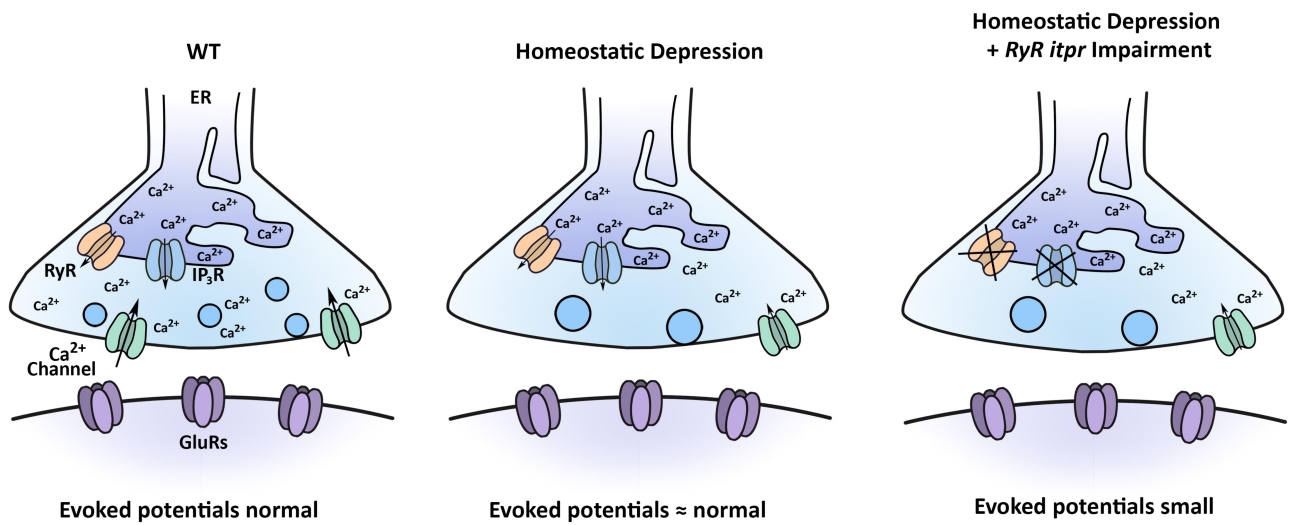
WT
ER
RyR
IP3R
Ca2+ Channel
GluRs
Evoked potentials normal
Homeostatic Depression
Evoked potentials ≈ normal
Homeostatic Depression
+ RyR itpr Impairment
Evoked potentials small